Forest Ecology and Management 520 (2022) 120355

Contents lists available at ScienceDirect

Forest Ecology and Management

journal homepage: www.elsevier.com/locate/foreco

Do mycorrhizal symbionts drive latitudinal trends in photosynthetic carbon use efficiency and carbon sequestration in boreal forests?

Annikki Mäkelä [a,b,*], Xianglin Tian [a,b], Anna Repo [c], Hannu Ilvesniemi [c], John Marshall [b], Francesco Minunno [a], Torgny Näsholm [b], Pauliina Schiestl-Aalto [a,b], Aleksi Lehtonen [c]

[a] Institute for Atmospheric and Earth System Research (INAR)/Forest Sciences, Helsinki 00014, Finland
[b] Department of Forest Ecology and Management, SLU, Umeå 901 83, Sweden
[c] Natural Resources Institute, Finland (Luke), 00791 Helsinki, Finland

ARTICLE INFO

Keywords:
Carbon allocation
Carbon residence time
Carbon use efficiency
Model
Mycorrhiza
Net ecosystem production
Soil C balance
Soil C:N ratio

ABSTRACT

There is evidence that carbon fluxes and stocks decrease with increasing latitude in boreal forests, suggesting a reduction in carbon use efficiency. While vegetation and soil carbon dynamics have been widely studied, the empirical finding that ectomycorrhizal fungi (ECM) become more abundant towards the north has not been quantitatively linked to carbon use efficiency. We formulated a conceptual model of combined fine-root and ECM carbon use efficiency (CUE) as NPP/GPP (net primary production/gross primary production). For this, we included the mycorrhiza as gains in plant NPP but considered the extramatrical hyphae as well as exudates as losses. We quantified the carbon processes across a latitudinal gradient using published eco-physiological and morphological measurements from boreal coniferous forests. In parallel, we developed two CUE models using large-scale empirical measurements amended with established models. All models predicted similar latitudinal trends in vegetation CUE and net ecosystem production (NEP). CUE in the ECM model declined on average by 0.1 from latitude 60 to 70 with overall mean 0.390 ± 0.037. NEP declined by 200 g m^{-2} yr^{-1} with mean 171 ± 79.4 g m^{-2} yr^{-1}. ECM had no significant effect on predicted soil carbon. Our findings suggest that ECM can use a significant proportion of the carbon assimilated by vegetation and hence be an important driver of the decline in CUE at higher latitudes. Our model suggests the quantitative contribution of ECM to soil carbon to be less important but any possible implications through litter quality remain to be assessed. The approach provides a simple proxy of ECM processes for regional C budget models and estimates.

1. Introduction

In boreal forests, measurements and models indicate that canopy photosynthesis (GPP) and other carbon fluxes decline with increasing latitude (Minunno et al. 2016, Ťupek et al., 2015, Vanhala et al. 2008). Similarly, carbon pools of upland soils and vegetation are reduced at higher latitudes (Lehtonen et al. 2016a). Assuming that the latitude-mean C pools are close to their steady states, the pool sizes can only decrease in the northward direction if the pool-specific rates at which carbon is returned to the atmosphere decrease less in that direction than those of GPP (Mäkelä et al. 2008). Increase of respiration, either autotrophic or heterotrophic or both, relative to GPP could therefore explain these observed trends in C pools. There is indeed evidence that GPP declines with mean annual temperature less than net primary production (NPP) (West 2020), suggesting that carbon use efficiency (CUE = NPP / GPP) should have a northward declining trend (DeLucia et al. 2007). Regarding heterotrophic respiration, soil carbon turnover rates are predicted by models to decrease northward due to lower temperatures and precipitation (Vanhala et al. 2008, Wang et al. 2017), but less is known about how this reduction relates to the observed trends in GPP.

Autotrophic respiration is reflected in vegetation CUE (*E*), as NPP is GPP less autotrophic respiration (Manzoni et al. 2018, West 2020). When construction respiration and maintenance respiration are considered separately, CUE can be expressed as (growth efficiency) × [1 – (maintenance respiration)/GPP] where growth efficiency indicates the relative carbon yield of growth after construction respiration. This can be further elaborated as follows:

---

* Corresponding author.
E-mail address: Annikki.makela@helsinki.fi (A. Mäkelä).

https://doi.org/10.1016/j.foreco.2022.120355
Received 7 January 2022; Received in revised form 2 June 2022; Accepted 8 June 2022

$$E = \frac{1}{1+c}\left[1 - \frac{r_f + r_r\left(\frac{W_r}{W_f}\right) + r_w\left(\frac{W_w}{W_f}\right)}{\sigma_C}\right] \tag{1}$$

where W_i is root ($i = r$), foliage (f) and sapwood (w) carbon content, σ_C is foliage specific mean annual rate of photosynthesis, r_i are mean annual organ-specific maintenance respiration rates and c is the proportion of carbon lost per one unit of carbon used in growth, termed construction respiration (Mäkelä and Valentine, 2001). Trends in E can emerge due to trends in construction respiration, in the ratio of maintenance respiration to foliage-specific photosynthetic rate, or in fine-root to foliage or sapwood to foliage ratio. While the rate of photosynthesis has been widely covered by literature based on decades of experiments and modelling (Ryu et al. 2019), and the biomass ratios are readily measurable (Helmisaari et al. 2007), rates of respiration still remain largely unknown. An increasing trend in the fine root to foliage ratio with latitude has been observed (Helmisaari et al. 2007, Lehtonen et al. 2016b) which could contribute to a declining northward trend in E, provided that an opposite trend did not exist in the sapwood to foliage ratio. Maintenance respiration rates have been related to temperature and tissue N content (Ryan et al. 1996, Collalti et al. 2020) but have also been found to vary in parallel with photosynthesis (Dewar et al. 1999, Wertin and Teskey 2008), rendering E relatively insensitive to the environment. If CUE really has a declining trend with latitude, some key elements seem to be missing from our conventional description of the production and consumption processes in forest ecosystems.

A key to this discrepancy could lie in the omission of fungal symbionts from the CUE analysis. Previous studies have indicated that in coniferous forests grown in nutrient-poor environments a lot of the assimilated carbon is directed below-ground to support ectomycorrhizal fungi (ECM; Högberg et al. 2001, Vicca et al. 2012). Although these fungi are technically heterotrophs, their reliance on symbiotic carbon from vegetation means they function like autotrophs. An increasing body of evidence suggests that the rates of respiration and turnover of ECM and the related extramatrical mycelium can be considerable in comparison with fine root respiration and turnover (Fitter 1991,Wallander et al. 2004, Ekblad et al. 2013, Hagenbo et al. 2019). A recent review of mycorrhizal colonization in boreal Norway spruce forests presented evidence that the rate of colonization of fine roots by ECM was related to the organic soil C:N ratio and increased with increasing latitude (Ostonen et al. 2011). A latitudinal trend in soil quality could therefore explain any concurrent trends in CUE through belowground allocation to ECM.

Inclusion of ECM in ecosystem carbon balance has implications on soil carbon and the related estimates of carbon residence time in soils. Firstly, the carbon allocated to ECM will produce microbial litter, creating a generally unaccounted input of carbon to the soil. Secondly, the properties of microbial litter are different from plant litter (Clemmensen et al. 2013). The decomposition process may be further enhanced through release of exudates that also prime the decomposition of soil organic matter by non-symbiotic organisms (Talbot et al. 2008, Adamczyk et al. 2019). Some mycorrhizal fungi can degrade recalcitrant organic matter, so they contribute to decomposition despite being fed plant C (Lindahl and Tunlid 2015). ECM activity could therefore underlie any trends, not only in CUE, but also in carbon residence time in the entire forest ecosystem.

The objective of this study is to explore the implications of the finding that ECM colonization increases with C:N ratio (Ostonen et al. 2011) on possible latitudinal trends of CUE and soil carbon dynamics in boreal forests. Based on this, we formulate a simple conceptual model of the combined carbon use of fine-root and ECM, and quantify it across a latitudinal gradient using published eco-physiological and morphological measurements from boreal coniferous forests. In parallel, we present two carbon use efficiency models using large-scale empirical measurements amended with established models where direct measurements cannot be obtained (Lehtonen et al. 2016a). In this study, we will focus on Finland where data and models are readily available to us. We aim to answer the following research questions: (1) Does our empirical data imply latitudinal trends in CUE and NEP? (2) Can ECM abundance explain these trends? (3) Under our stated premises, what is the quantitative significance of ECM on CUE, NEP and soil carbon accumulation?

2. Material and methods

2.1. The ECM model

2.1.1. Formulation

Here we develop a model that will allow us (1) to modify Eqn (1) so as to incorporate the effect of ECM on vegetation CUE, and (2) to consider the impacts of ECM on the soil organic carbon balance. The model considers the allocation of below-ground carbon flux to roots, mycorrhiza, the extramatrical mycelium and root exudates. The turnover of the extramatrical mycelium produces fungal litter that is added to the plant litter input to the soil. Exudation may prime the decomposition processes (Fig. 1).

We consider the “standing biomass” (per unit land area, g C m^{-2}) of ectomycorrhizal fungi to include both mycorrhizae (M) and the extramatrical mycelium (H, including sporocarps). We express M as a proportion, ρ_M, of the uncolonised fine root biomass W_r(g C m^{-2}) and H as a proportion, h_M, of M (Table 1, Table 2).

When fine root biomass is measured, it usually includes the biomass of ectomycorrhizal symbionts of the root tips which cannot be separated from fine root mass. We denote the combined root-fungal mass by W_{RT}, such that $W_{RT} = (1+\rho_M)W_r$. This allows us to relate the total fungal mass, $M + H$, to the combined root-fungal mass, W_{RT} (Table 1, Table 2).

The carbon consumption of ECM consists of their growth and respiration. The carbon input to the soil by ECM consists of their litter production and exudation. Here, we develop simple, “0 order” expressions for the mean annual rates of all these processes, with the objective of analyzing the significance of ECM carbon consumption for plant and soil C balance. Here we briefly state our concepts and assumptions, the exact forms of which can be found in Table 1.

For the maintenance respiration of all components, M, H, and W_r, we follow the conventional model where respiration rate is proportional to component biomass, assigning annual specific mean rates r_M, r_H and r_r to the components, respectively. Analogous to respiration, we attach annual mean turnover rates s_M, s_H and s_r to the components (Table 1, Table 2).

For estimating carbon allocation to ECM growth and construction respiration, we shall assume that the ECM system is approximately at steady state. Although clearly not a fully accurate assumption, this will nevertheless allow us to estimate the order of magnitude of the C flux consumed in ECM construction. In steady state, growth is equal to turnover, and the total carbon used by fungal production is growth plus construction respiration, where all components are assigned their own rates of construction respiration. These are denoted by c_r, c_M, and c_H for uncolonized fine roots, colonized root tips and extramatrical hyphae, respectively (Table 1, Table 2).

Part of the sugars transported to the roots and hyphae may just leak out as exudates, without being used by fine roots or ECM. The mechanisms of exudation are not fully understood (Canarini et al. 2019), but there is evidence that while exudation through root tips may decline with ECM colonization, additional exudation simultaneously takes place through the hyphal network (Gorka et al. 2019). We therefore assume, for consistency with the rest of the model, that the rate of exudation increases with the rate of ECM colonization. We denote the relative rate of exudation per colonized root tips by ξ (Table 1, Table 2).

The exudates leaked through the symbionts may stimulate the SOM decomposition rate by heterotroph microbes in the soil. We assume that this increase of SOM decomposition is proportional to the release of exudates, with parameter ϕ_M indicating the (mean annual) specific rate

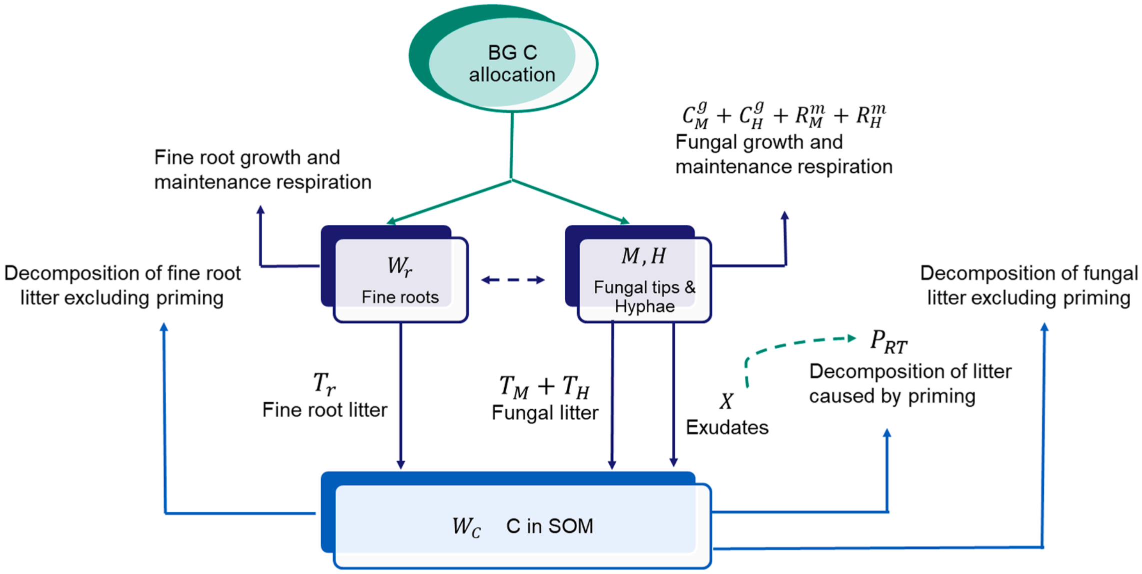

Fig. 1. A schematic presentation of the below-ground contribution to the carbon balance of the vegetation-ectomycorrhizae (ECM) system. The boxes represent dynamic carbon storages and the solid arrows represent fluxes. The dashed arrows indicate impacts. The symbols are as in Table 1.

Table 1
ECM model state (S) and rate (R) variables and their definitions. All states are expressed in g C m^{-2} and all rates are in g C m^{-2} yr^{-1}. The specific rate parameters in the definition column are specified in Table 2.

Symbol	Meaning	Definition	Type
W_{RT}	Fine root + fungal mass in colonized tips	$W_{RT} = W_r + M$	S
W_r	Bare part of fine roots	$W_r = \frac{1}{1+\rho_M} W_{RT}$	S
M	Mass of colonized tips	$M = \rho_M W_r$	S
H	Mass of extramatrical fungi	$H = h_M \rho_M W_r$	S
R_{RT}^m	Maintenance respiration of fine root + fungal mass in colonized tips	$r_{RT} W_{RT} = \frac{r_r + \rho_M r_M}{1+\rho_M} W_{RT}$	R
R_r^m	Fine root maintenance respiration	$r_r W_r$	R
R_M^m	Maintenance respiration of fungal tips	$r_M M$	R
R_H^m	Maintenance respiration of extramatrical fungi	$r_H H$	R
T_{RT}	Fine root + fungal tips turnover rate	$s_{RT} W_{RT} = \frac{s_r + \rho_M s_M}{1+\rho_M} W_{RT}$	R
T_r	Fine root turnover rate	$s_r W_r$	R
T_M	Turnover rate of fungal tips	$s_M M$	R
T_H	Turnover rate of extramatrical hyphae	$s_H H$	R
G_M	Growth of fungal tips at steady state	$G_M = T_M$	R
G_H	Growth of extramatrical hyphae in steady state	$G_H = T_H$	R
C_M^g	C consumption for constructing fungal tips	$(1 + c_M) G_M$	R
C_H^g	C consumption for constructing hyphae	$(1 + c_H) G_H$	R
X	Exudation	ξM	R
P_{RT}	Priming	$\phi_M X$	R

of priming per unit released exudates (Table 1, Table 2).

2.1.2. Carbon use efficiency

To modify Eqn (1) to include ECM impacts (Fig. 1), we shall investigate how the carbon allocated to ECM affects the CUE of the vegetation. For this, we consider the fine root – mycorrhizal complex as part of the plant and the extramatrical mycelium and exudates as external to the plant. The former is therefore included as gains in plant NPP but the latter taken as losses. This helps connect the results with root measurements that usually include the mycorrhiza but exclude the extramatrical mycelium.

To derive CUE, we express GPP as the sum of its component uses for

Table 2
Reference values for metabolic parameters. Variation of parameter values specified as "default assumption" will be explored in more detail (see Table 5).

Parameter	Meaning	Units	Range	Reference
h_M	extramatrical hyphal biomass parameter	–	0.14 ± 0.04	Hagenbo et al. 2019
γ	apparent hyphal respiration rate	yr^{-1}	2.66 ± 0.5	Hagenbo et al. 2019
s_H	hyphae specific turnover rate	yr^{-1}	2.0 ± 1.0	Hagenbo et al. 2019
ϕ_M	priming parameter	–	1 ± 0.5	default assumption
σ_C	mean foliage-specific annual rate of photosynthesis pine / spruce	yr^{-1}	3.4–4.0/ 2.2–2.6	Schiestl-Aalto et al. 2019 / SMEAR II
r_f	mean foliage-specific annual rate of maintenance respiration	yr^{-1}	0.63 ± 0.06	Schiestl-Aalto et al. 2019 / SMEAR II
r_r	mean fine-root specific annual rate of maintenance respiration	yr^{-1}	0.53 ± 0.05	Schiestl-Aalto et al. 2019 / SMEAR II
r_w	mean sapwood-specific annual rate of maintenance respiration	yr^{-1}	0.037 ± 0.004	Schiestl-Aalto et al. 2019 / SMEAR II
c	mean construction respiration of vegetation	–	0.3 ± 0.03	Penning de Vries 1972
r_R	mean root-tip annual rate of maintenance respiration		0.53 ± 0.05	default assumption
c_R	mean construction respiration of fungal root tips		0.3 ± 0.03	default assumption
s_r	fine root turnover rate	yr^{-1}	1.0 ± 0.5	Leppälammi-Kujansuu (2014)
s_R	turnover rate of the colonized root tips	yr^{-1}	1.0 ± 0.5	default assumption
ξ	rate of exudation	yr^{-1}	0.5 ± 0.5	default assumption

plants and ECM as follows:

$$P = (1+c)G_V + R_V^m + (1+c_M)G_M + (1+c_H)G_H + R_M^m + R_H^m + X \tag{2}$$

where P is GPP, G_V is plant production (NPP of plants excluding colonized root tips), R_V^m is plant maintenance respiration, and c is the proportion of NPP lost as plant construction respiration. The terms related to carbon used by the colonized tips and hyphae are construction costs ($(1+c_M)G_M$ and $(1+c_H)G_H$, respectively), maintenance respiration rates (R_M^m and R_H^m, respectively), and exudation (X) (see also Table 1).

Starting from Eqn (2), a modified Eqn (1) can now be derived (For derivation see Supplementary Material, SM1). In the resulting formula (Fig. 2), an additional fungal consumption term has been added to the fine root respiration term. It includes the carbon consumed in fungal growth, maintenance and exudation, separating between cases when the bare fine roots and colonized root tips are assumed to have either the same or different rate parameters.

2.1.3. Carbon residence time in soil and NEP

The fungal litter constitutes an additional input of carbon to the soil which is often not explicitly included in state-of-the-art soil carbon models (Viskari et al. 2020, but see Wieder et al. 2015) but has a tendency to increase the soil carbon pool. The net effect depends on the relative sizes of the litter and priming fluxes. To what extent do the extra litter input and priming balance each other out, and does this balance differ between environments and ecosystems? We shall consider these questions using a simple steady-state approach.

First, consider the system in the absence of extramatrical hyphae and priming, and assume that the colonized and uncolonized roots share their turnover rate, $s_r = s_M$. The rate of change of the soil carbon pool, W_C, is then expressed as.

$$\frac{dW_C}{dt} = L_{AGC} + s_{RT}W_{RT} - \frac{1}{\tau}W_C \tag{3}$$

where L_{AGC} is carbon in above-ground and coarse-root litter fall, and τ is the mean residence time of carbon in the soil assuming no priming. Steady state soil carbon (SSSC) is thus.

$$\overline{W}_{C1} = \tau(L_{AGC} + s_{RT}W_{RT}) \tag{4}$$

where $\overline{W}_{C1}$ refers to the steady state value without explicitly considering ECM litter. The corresponding steady-state heterotroph soil respiration is equal to the litter input from above- and below-ground vegetation:

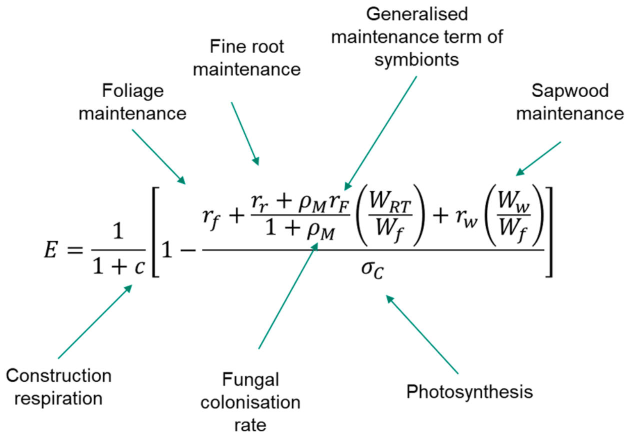

$$E = \frac{1}{1+c}\left[1 - \frac{r_f + \frac{r_r + \rho_M r_F}{1+\rho_M}\left(\frac{W_{RT}}{W_f}\right) + r_w\left(\frac{W_w}{W_f}\right)}{\sigma_C}\right]$$

Fig. 2. Equation *(1)* modified to include ECM. Here, ρ_M is the colonization rate of ECM and r_F is the combined fungal C consumption rate, defined as $r_F = (\Delta_M + (1+c_H)h_M s_H + r_M + h_M r_H + \xi)$. Δ_M represents the impact of different construction respiration and turnover rates of fungi and fine roots, $(1+c_H)h_M s_H$ is the construction cost of extramatrical mycelia, r_M and $h_M r_H$ are maintenance costs of colonized tips and extrametrical mycelia, respectively, and ξ is the specific rate of exudation. Other symbols as in Eqn (1) and Table 1.

$$\overline{R}_{HSS1} = L_{AGC} + s_{RT}W_{RT} \tag{5}$$

Adding the flux of carbon through ECM litter ($\Delta s_M M + T_H + X$) and the related priming (P_{RT}) in the rate equation yields:

$$\frac{dW_C}{dt} = L_{AGC} + s_{RT}W_{RT} + \Delta s_M M + T_H + X - \frac{1}{\tau}W_C - P_{RT} \tag{6}$$

where T_H, X and P_{RT} are defined in Table 1 and the Δs_M-term represents the possibly faster turnover of the colonized root tips that was not accounted for in the fine-root turnover term $s_r W_{RT}$. Using the definitions of Table 1, we can solve for SSSC:

$$\overline{W}_{C2} = \tau\left(L_{AGC} + s_{RT}W_{RT} + \frac{\rho_M s_F}{1+\rho_M}W_{RT} - P_{RT}\right) \tag{7}$$

where $\overline{W}_{C2}$ refers to the steady state when the fungal processes have been explicitly included. Here we have denoted by s_F the combined additional fungal turnover and exudation: $s_F = (\Delta s_M + h_M s_H + \xi)$.

Eqn (7) quantifies the change of SSSC that has a tendency to increase due to increased fungal litter input but to decrease due to priming by ECM. The corresponding steady state heterotroph respiration equals litter input plus exudation:

$$\overline{R}_{HSS2} = L_{AGC} + s_{RT}W_{RT} + \frac{\rho_M s_F}{1+\rho_M}W_{RT} \tag{8}$$

The actual mean residence time of carbon in soil, accounting for the priming by exudates, can now be calculated, according to its definition, as the ratio of SSSC and steady state respiration rate:

$$\tau' = \frac{\overline{W}_{C2}}{\overline{R}_{HSS2}} \le \tau \tag{9}$$

Eqn (9) implies that whenever priming occurs ($\xi\phi_M > 0$), the actual residence time must be smaller than the residence time under no exudation. Furthermore, if priming is so strong that $\xi\phi_M > \Delta s_M + h_M s_H + \xi$, i.e., if the exudates stimulate enough microbial activity to compensate for the carbon input by microbial litter, the microbial litter production minus priming in Eqn (7) would be negative, leading to a reduction of SSSC in comparison with Eqn (4).

The effects of ECM on CUE and carbon residence time (τ) in soil can be summarized as the corresponding effect on NEP if ecosystem production, GPP, and soil carbon content are known:

$$NEP = EP - \frac{1}{\tau}W_C \tag{10}$$

where P refers to GPP, EP is NPP, and $\frac{1}{\tau}W_C$ approximates heterotroph respiration either with ($\tau = \tau'$) or without ($\tau = \tau$) ECM effects.

2.2. Quantifying the model across a latitudinal gradient

2.2.1. Method overview

Our country-wide calculation network was based on the sample plots of the Biosoil data set, collected by EU-wide Forest Focus monitoring project during 2006–2007 (ICP Forests Level I). The data set consists of over 600 sample plots across Finland, measured for stand characteristics and soil properties and combined with climatic variables from local weather stations. Measured soil properties include soil carbon and nitrogen content separated to organic and mineral layers. The sampling was based on the Finnish NFI grid (Tomppo et al. 2011) that has been used for permanent sample plots measured from 1985 (Mäkipää and Heikkinen 2003). We used all conifer-dominated Biosoil sites (conifer share of basal area greater than 50%). For more details, see Heiskanen et al. (2018) and SI2.

To quantify the model, we need inputs of (1) tissue-specific metabolic rates for trees and ECM, (2) biomass ratios, and (3) values of fluxes and stocks. We make the following "zero order" assumptions (Fig. 3):

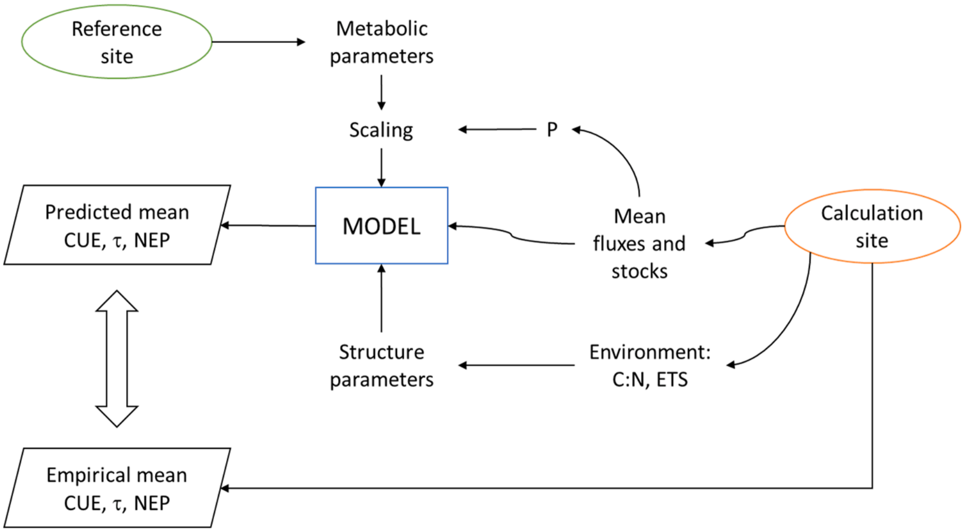

Fig. 3. A schematic presentation of the approach of the study. We use reference site data from the literature to estimate metabolic parameters of the model, scale these up using relative photosynthesis rates (P), and estimate structure parameters using C:N ratio and effective temperature sum (ETS) of each calculation site. We estimate additional mean fluxes and stocks for the calculation sites to obtain regional estimates of model inputs and hence model predictions. We use empirically defined methods to provide alternative regional estimates of the output variables.

1. Mean annual tissue-specific metabolic rates are estimated for a reference site and scaled to country level using photosynthesis rates. This is based on the finding that the key source of latitudinal variation of metabolic rates in boreal forest is growing season length which is also reflected in GPP (Mäkelä et al. 2008, Härkönen et al. 2010).
2. The latitudinal variation of biomass ratios is controlled by environmental drivers. We assume that the C:N ratio of soil organic layer determines both ECM colonization rates (Ostonen et al. 2011) and fine root to foliage ratios (Helmisaari et al. 2007). The sapwood to foliage ratio is largely determined by tree height (Mäkelä and Valentine, 2001) which decreases, on average, from south to north. We derive this from Effective Temperature Sum (ETS, sum of daily temperatures exceeding 5 °C).
3. The fluxes and stocks occurring in the equations can be treated as long-term mean values and estimated as regional means *i.e.*, using the space-for-time approximation (Picket 1989).

Using the above assumptions, we describe below how we collected the relevant data and evaluated the model across the Biosoil network, to reveal any trends in the estimated variables.

2.2.2. *Metabolic parameters at reference sites*

We used published results from the SMEAR II station, Hyytiälä, Finland (61°51′N, 24°17′E), to determine the reference parameters related to vegetation photosynthesis and respiration (Schiestl-Aalto et al. 2019; Minunno et al. 2016). Our main source for estimating the reference parameters related to the ECM processes was the study by Hagenbo et al. (2019), who investigated the significance of extramatrical mycelia in the carbon balance of a chronosequence of Scots pine stands in central Sweden. The location and type of the sites is comparable to the SMEAR II station, with sandy podzolic soils, growing season length around 170–180 days (mean daily temperature consecutively over 5 °C), and site indices (H_{100}, dominant height at age 100 yrs) ranging from 24 to 27 m. The C:N ratio was not available for the Swedish sites, so we assumed it to be the same as for SMEAR II.

A key result of the ECM study for our analysis was the estimation of the mean respiration rate attributable to extramatrical hyphae. As a caveat of this measurement Hagenbo et al. (2019) identified the possibility that some of the measured respiration originated in priming rather than hyphal respiration. We define parameter γ as this combined respiration, yielding (see Table 1):

$$[h_M(c_H s_H + r_H) + \xi\phi_M]\frac{\rho_M}{1+\rho_M}W_{RT} = \gamma\frac{\rho_M}{1+\rho_M}W_{RT} \tag{11}$$

We analysed the role of priming by (1) varying the share of priming, $\xi\phi_M$, in the above sum, and alternatively, (2) by adding priming on top of the estimated total respiration, to explore the possibility that not all priming was included in γ. See SM3 for details of parameter estimation and Table 2 for the estimated values.

2.2.3. *Environmentally-driven structure parameters*

To estimate the colonization rate of ECM in fine roots, ρ_M, we used the study by Ostonen et al. (2011) that covers boreal spruce forests from Estonia to Finnish Lapland. We used their data to estimate the dependence of ρ_M on organic layer C:N ratio (Ostonen et al. 2011) (SM4, Fig. 4).

For the dependence of fine root to foliage ratio on organic layer C:N ratio, we fitted an exponential function to data in Helmisaari et al. (2007), separately for spruce and pine (SM4, Fig. S4.1a).

For estimating the sapwood-to-foliage biomass ratio, we used national statistics from NFI11 (https://urn.fi/URN:ISBN:978–952-326–467-0) of woody biomass and foliage biomass, separately for spruce and pine. We assumed that 60% of stem biomass and 90% of live branch biomass and all root biomass minus stump is sapwood (Vanninen and Mäkelä 2005). The regional values were allocated to the Biosoil sites of each region and assigned a mean ETS of the respective Biosoil sites. Exponential functions were fitted to estimate

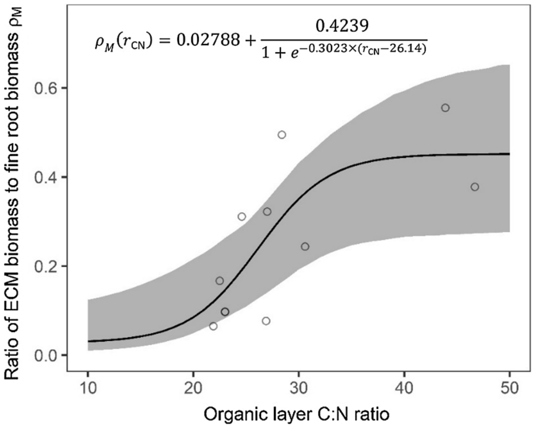

Fig. 4. Dependence of relative ECM abundance on C:N ratio. Circles are measurements from Ostonen et al. (2011). The line was generated by fitted model and MAP (the maximum a posterior parameter vector). The grey area represents the 95% Bayesian credible interval based on parametric uncertainty.

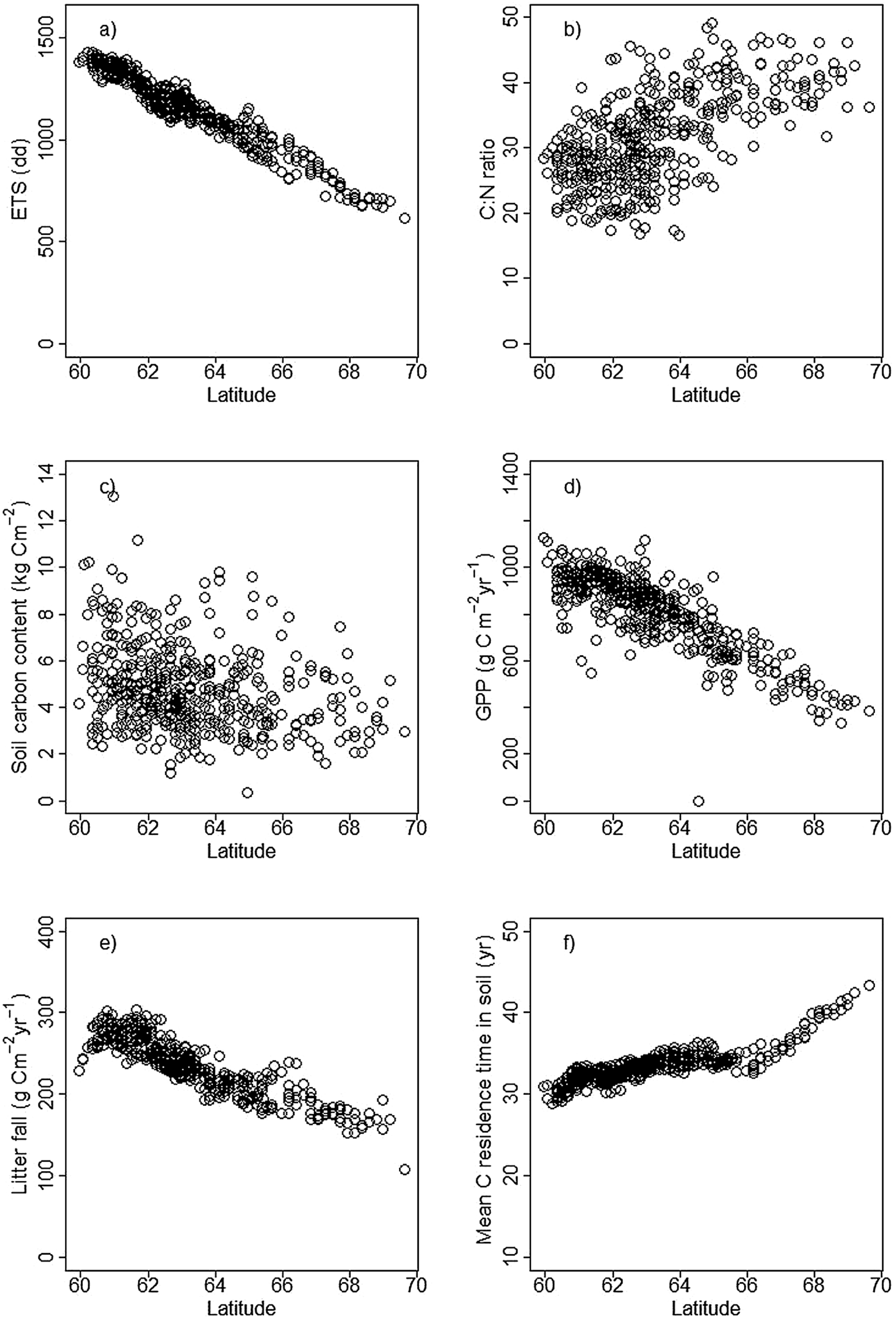

Fig. 5. Latitudinal trends of model inputs at Biosoil sites ($n = 434$). a) Effective temperature sum (ETS), b) organic layer C:N ratio (not available at all sites), c) soil C content of non-peatland soils, d) ecosystem mean GPP estimated with MODIS GPP product, e) total litter fall from the gridded litter fall data set, f) Mean residence time τ of soil carbon as calculated with Yasso15 using the litter fall data from the gridded litter fall data base.

W_w/W_f from ETS (SM4, Fig. S4.1b).

2.2.4. Mean fluxes and stocks at calculation sites

For calculating soil C and NEP (Eqns. (3)–(10)) we needed data on 7 variables (Table 3). The Biosoil sites (Fig. S2.1) provided direct measurements for r_{CN}, D and W_C. Ecosystem GPP was estimated for the Biosoil sites using the MODIS web service (Running et al. 2004, https://modis.gsfc.nasa.gov/data/dataprod/mod17.php). The MOD17A2H GPP product is a cumulative 8-day composite of values with 500-m pixel size (Running et al. 2015). For every 8th day of the year, we estimated the mean photosynthesis after deleting no-data values for the period 2001–2020, and then aggregated daily photosynthesis to obtain mean annual GPP for these 20 years.

Above- and below-ground litter fall estimates came from a gridded litter fall data set for Finland (Lehtonen et al. 2016a), including litter fall components of living trees, understory and harvest residues. The litter fall data was available on a 10 x10 km^2 grid across Finland and was allocated to the Biosoil sites according to the grid where the site was

Table 3
Variables estimated for scaling the results.

Variable	Meaning	Units	Source
r_{CN}	C:N ratio of organic layer	$\mathrm{g\ C\ g^{-1}N}$	Biosoil data
D	Effective temperature sum (ETS)	^{o}Cd	Biosoil data
P	ecosystem photosynthesis (GPP)	$\mathrm{g\ C\ m^{-2}\ yr^{-1}}$	MODIS around Biosoil sites
L_{AGC}	litterfall excluding fine roots	$\mathrm{g\ C\ m^{-2}\ yr^{-1}}$	Gridded litterfall data
τ	carbon residence time in soil - reference	yr	Yasso15 with gridded litterfall and weather data
W_C	soil carbon	$\mathrm{g\ C\ m^{-2}}$	Biosoil data
W_{RT}	root biomass	$\mathrm{g\ C\ m^{-2}}$	Lehtonen et al. 2016b

located. For more details, see Lehtonen et al. (2016a) and SM2.

τ was estimated by applying the gridded litter fall data as input to a soil carbon model, Yasso15 (Viskari et al., 2020). Yasso is a process-based model where the decomposition rate of soil C depends on the chemical composition of litter and on air temperature and precipitation. The decomposition of woody litter also depends on litter diameter (Tuomi et al., 2011). Yasso15 has been parametrized on a diverse dataset of measurements of non-woody and woody litter decomposition, soil carbon stocks and soil carbon accumulation (see https://en.ilmatieteenlaitos.fi/yasso, SM2), advancing from its previous version Yasso07 (Tuomi et al., 2011, 2008).

We estimated long-term mean fine-root biomass (g C m^{-2}) from stand basal area (G) and organic layer C:N ratio using a model developed by Lehtonen et al. (2016b):

$$W_{RT} = 1.114G^{0.734}r_{CN}^{0.721} \tag{12}$$

Here (G) was the long-term mean basal area retrieved by region from forest statistics (NFI11).

All model input variables (Table 3) correlated significantly with latitude (Fig. 4). Linear correlations were strongest for ETS and ecosystem GPP and weakest for soil carbon content.

2.3. *Estimating CUE and NEP empirically from regional data*

For estimating empirical latitudinal trends of CUE and NEP, we derived two different methods based on carbon balance. The underlying assumption in both methods was to consider trends in long-term average fluxes and stocks, some of which can be estimated using the space-for-time substitution (Picket 1989). We first estimated CUE, then calculated NEP by inserting CUE in Eqn (10). Here we describe the main assumptions and data behind the estimates. For details see SM5.

2.3.1. *Method 1.*

The long-term mean GPP of the Biosoil sites was estimated from MODIS. The long-term mean NPP estimate ($\widehat{P}_N$) was calculated assuming that (1) woody growth is proportional to stem growth, and (2) non-woody growth equals non-woody litter fall, because foliage, fine roots and ground vegetation show steady values in mature stands that represent the main part of all stands. Therefore,

$$\widehat{P}_N = a\widehat{G}_W + L_{nw} \tag{13}$$

where $\widehat{G}_W$ is stem biomass growth, a converts that to total woody biomass growth and L_{nw} is non-woody litter fall. Woody biomass growth was estimated based on NFI11, and non-woody litter fall came from the gridded litter fall data set.$\widehat{P}_N$ was divided by GPP to estimate CUE.

2.3.2. *Method 2*

We derived another, indirect method for estimating CUE from statistics and the soil carbon pool, utilizing the mean residence time of carbon in the soil, τ, predicted by Yasso15. The annual rate of accumulation of carbon in the ecosystem over time interval $[t-T,t]$, split into vegetation (W_v) and soil carbon (W_C), is.

$$\frac{dW_v}{dt} + \frac{dW_C}{dt} = EP - H - \frac{W_C}{\tau} \tag{14}$$

where H denotes annual harvests. Integrating both sides over the time interval $[t-T,t]$, dividing by the length of the interval, T, and solving for long-term mean CUE (E) yields:

$$E = \frac{1}{P}\left[\frac{W_C(t)}{\tau} + \widehat{H} + \gamma_v - \gamma_s\left(\frac{T}{2\tau} - 1\right)\right] \tag{15}$$

where $\gamma_i = \frac{\Delta W_i}{T}\,(i = v, C)$ is the mean annual net change in the vegetation and soil carbon pools.

For quantifying E of Eqn (15), we used soil C from the Biosoil measurements and τ from the Yasso15 simulations. The mean harvests were computed by forestry region from national statistics, and the change in forest biomass was calculated from a national trend of stem wood volume (NFI11). The temporal trend of soil carbon was obtained from a study on the Biosoil sites (Kramarenko 2012).

2.4. *Simulation, sensitivity and uncertainty analyses*

Using the model across the Biosoil network, we conducted simulations to assess if there were latitudinal trends in CUE, τ and NEP, and compared these with the respective empirically-based trends. Regarding the ECM carbon balance, we analysed six alternative assumptions on parameter values (Table 4). For uncertainty analysis we used a variance-based uncertainty partitioning approach to attribute the uncertainty of CUE estimates to different parameters and modules (SM6).

3. Results

3.1. *Measurement-based trends in CUE, soil residence time and NEP*

Both our empirical-based methods predicted significant trends of CUE with latitude and ETS, but the mean CUE values were higher (0.446 ± 0.064 *vs* 0.370 ± 0.082) and the trend was weaker in method 1

Table 4
Sensitivity tests performed with the model.

Name of test	Meaning	Method
No ECM	Reference model performance with no ECM	$\rho_M = 0$
Default	- Colonized root tips show the same respiration and turnover rates as bare roots - Priming is included in total respiration γ	Parameter values as in Table 2
Roots constant	Assuming constant root biomass instead of C:N dependence (Eqn (12))	$W_{RT} = 106\ \mathrm{g\ C\ m^{-2}}$
1.2 γ / 0.8 γ	Testing the basic sensitivity to the assumed level of respiration + exudation (Eqn (11))	γ is varied by ±20%
Double ECM metabolism	Testing the effect of faster metabolism of fungal component in colonized root tips	Doubled values of r_R, c_R and s_R
Total respiration constrained by γ	Assuming fixed hyphae-specific C losses, γ, the share of fungal respiration and priming in γ is varied	ξ and ϕ_M vary in Eqn (11) while γ remains fixed
ECM respiration constrained, priming added	Priming is additional to the estimated total hyphae-specific C losses, γ	ξ and ϕ_M vary in Eqn (11) while $h_M(c_H s_H + r_H)$ remains fixed

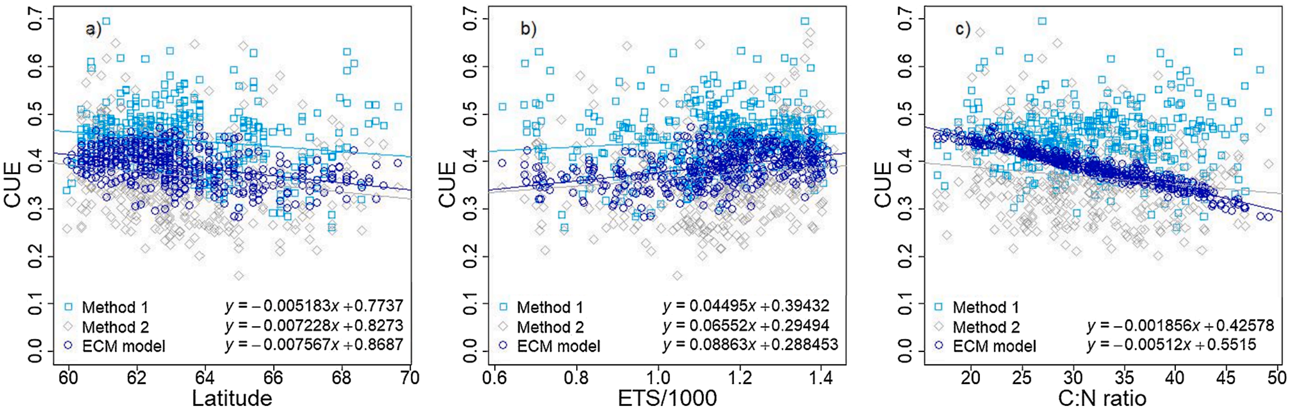

Fig. 6. Carbon Use Efficiency of vegetation (CUE) predicted using the ECM allocation model, empirical method 1 and empirical method 2. a) CUE against latitude. All trends are significant ($p < 0.001$). b) CUE against ETS/1000. Model:$p < 0.001$; Method 1: $p = 0.0108$; Method 2:$p = 0.00347$. c) CUE against C:N ratio of organic layer. Model:$p < 0.001$; Method 1: $p = 0.901$, Method 2: $p < 0.001$.

(Fig. 6a, 6b). Method 2 showed a significant trend with organic layer C:N ratio whereas method 1 did not (Fig. 6c). Both methods showed significant trends in NEP with respect to all explanatory variables (Fig. 7), with Method 1 producing larger values. NEP estimates ranged from 0 to 400 g C m^{-2} yr^{-1} (the system was sequestering C). The default τ, predicted by Yasso15 linked with our gridded litter fall data, had an increasing trend with latitude, varying between 30 and 45 yr. SSSC exceeded the measured average by 2 – 3 kg C m^{-2} but showed a similar trend with latitude (Fig. 8).

3.2. Trends predicted by the ECM model

3.2.1. Trends in the absence of ECM

Simulations in the absence of ECM ($\rho_M = 0$) gave significant but negligible trends for CUE of both spruce and pine with respect to latitude, ETS and organic layer C:N ratio ($p < 0.001$). The average CUE for pine was 0.53 ± 0.0131 and for spruce 0.48 ± 0.0054. The differences between minima and maxima were 0.058 and 0.024 for pine and spruce, respectively. In contrast, NEP had a significant ($p < 0.001$) and considerable declining trend in the absence of ECM with respect to all three variables. The mean was 271 ± 79 g C m^{-2} yr^{-1}, with maximum 466 and minimum 57 g C m^{-2} yr^{-1}.

3.2.2. Default trends compared with empirical estimates

With our default parameters, CUE varied between 0.26 and 0.49 with mean 0.390 ± 0.037, showing a significant declining trend with latitude, ETS and C:N ratio. The trends with latitude and ETS were somewhat stronger and with C:N ratio considerably stronger than those in the data-based estimates (Fig. 6, S7.1).

The average NEP estimate showed a similar range of values with Method 2, mostly varying from 50 to 250 g C m^{-2} yr^{-1} (Fig. 7, S7.2). Significant trends were detected with latitude, ETS and C:N ratio, with a slightly stronger trend in the model prediction than the data-based estimates especially with respect to C:N ratio.

The default simulation reduced τ by 2 to 3 years in comparison with the Yasso15 prediction and very slightly reduced the trend with latitude. The mean SSSC was about 0.1 kg C m^{-2} smaller, respectively (Fig. 8).

The cost of extramatrical hyphae and exudation (the components of ECM not embedded in fine roots) relative to photosynthesis increased from south to north, reaching a level of approximately 15%-20% when CUE was about 35% (Fig. 9a). The absolute average was 94 ± 37 g C m^{-2} yr^{-1}, compared with the mean GPP of 789 ± 185 g C m^{-2} yr^{-1}. The additional C inputs to soil, i.e. hyphal litter production and exudation, remained <10% of the heterotroph respiration at steady state ($\overline{R}_{HSS2}$), whereas the additional hyphal respiration together with added heterotroph respiration due to priming increased towards the north, reaching a maximum of approximately 40% of $\overline{R}_{HSS2}$ (Fig. 9b). The corresponding mean hyphal litter production (and growth, due to the steady-state assumption) was 8.9 ± 3.5 g C m^{-2} yr^{-1}.

3.2.3. Uncertainties in latitudinal trends

Under the default assumption of fixed total hyphal respiration γ, the latitudinal trend of CUE was strongest when colonized root tips were assigned faster metabolic rates than bare roots. The assumptions of increased total respiration and weaker priming also increased the slope, whereas attributing a larger proportion of total respiration to priming or

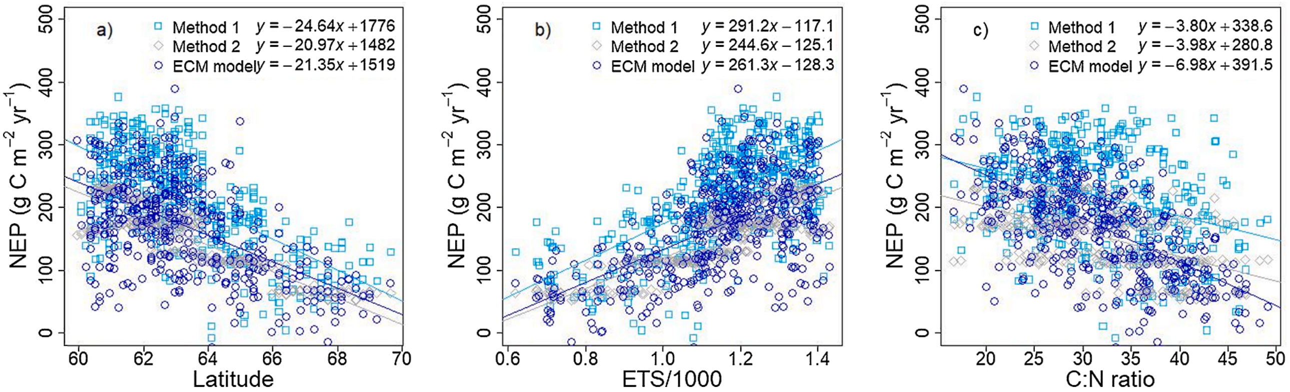

Fig. 7. Net Ecosystem Production (NEP) predicted using the ECM allocation model, empirical-based method 1 and empirical-based method 2. a) NEP against latitude. b) NEP against ETS/1000. c) NEP against C:N ratio of organic layer. All trends are significant ($p < 0.001$).

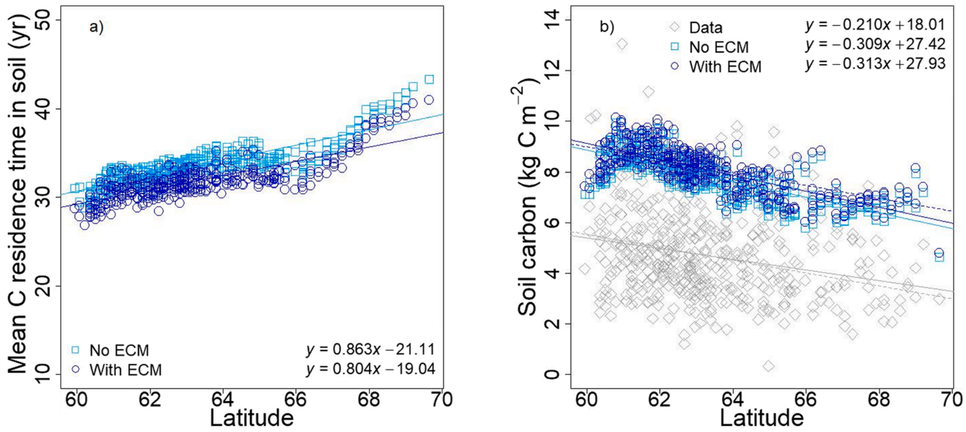

Fig. 8. a) Mean residence time as predicted by Yasso15 ($r^2 = 0.73$) and the default simulation ($r^2 = 0.52$) as functions of latitude. b) Steady-state soil carbon predicted by Yasso15 ($r^2 = 0.55$) and as modified by the default simulation ($r^2 = 0.52$), compared with measured soil carbon at the Biosoil sites ($r^2 = 0.06$). The dashed lines show a regression where a shared slope with different intercepts was fitted to the default model results combined with the data. The intercept was statistically significantly different between the two data sets ($t = 40.07$, $p < 0.001$).

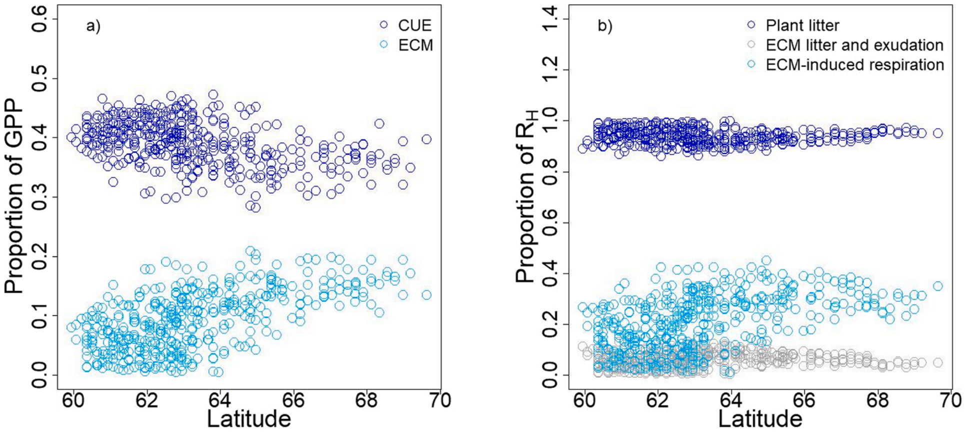

Fig. 9. Latitudinal trends in relative carbon fluxes. a) Proportions of GPP used for plant growth (=CUE) and for supporting ECM processes, b) Carbon fluxes into and out of the soil relative to total steady-state heterotroph respiration: plant litter production, ECM-originated inputs (including litter and exudation), and ECM-induced additional respiration (including hyphal growth and maintenance respiration and additional heterotroph respiration due to priming).

assuming 20% lower total respiration reduced the trend of CUE (Table 5).

The impact of the alternative assumptions on NEP, mean residence time of C in soil, and SSSC was generally small (Table 5). Increasing total respiration, assuming different ECM and root metabolism, and increasing exudation reduced the average NEP the most, but consistently $<10\%$. When total respiration was reduced, average NEP increased. The largest effect on τ was a reduction by 1.5 years, obtained assuming doubled exudation. Regarding SSSC, the only considerable difference (+0.85 kg m^{-2}) occurred under the assumption of different ECM and root metabolism, because the faster turnover rate of colonized roots under this assumption increased the litter input to the soil.

Table 5
Sensitivity of results to assumptions (See Table 4). For CUE, the table reports the slope (and its standard error) of the linear regression with respect to latitude. For NEP, τ, SSSC and ECM litter (Litter), we report the mean across all sites for the default simulation, and for other simulations, we report the simulation result minus the default value.

Assumption		**CUE**	**NEP** g C m^{-2} yr^{-1}	**τ** yr	**SSSC** kg C m^{-2}	**Litter** g C m^{-2} yr^{-1}
Total respiration constrained by γ	default	− 0.007567 (0.00080)	171 (79.4)	31.82 (2.10)	8.10 (0.86)	7.18 (3.02)
	roots constant	− 0.007567 (0.00080)	+0.1	+0.02	−0.01	−0.19
	1.2γ	−0.009558 (0.00092)	−9.6	0	0	0
	0.8γ	−0.005575 (0.00068)	+9.6	0	0	0
	double ECM activity	−0.010231 (0.00096)	−9.0	+0.2	+0.85	+25.6
	priming × 0.5	−0.008502 (0.00085)	−0.8	+0.8	+0.21	0
	priming × 1.5	−0.006631 (0.00074)	+0.6	−0.8	−0.21	0
	exudation × 2	−0.007567 (0.00080)	−7.1	−1.5	0	0
No ECM		ns	+0.66	+1.7	−0.24	−7.18
ECM respiration constrained, priming added	default parameters	−0.009438 (0.00091)	−9.1	0	0	0
	1.2γ	−0.011428 (0.0010)	−18.7	0	0	0
	0.8γ	−0.005575 (0.00068)	+0.6	0	0	0
	double ECM activity	−0.01210 (0.00108)	−18.1	+0.2	+0.85	+25.6
	priming × 0.5	−0.009438 (0.00091)	−5.4	+0.8	+0.21	0
	priming × 1.5	−0.009438 (0.00091)	−12.9	−0.8	−0.21	0
	priming × 3	−0.009438 (0.00091)	−26.2	−3.3	−0.85	0
	exudation × 2	−0.01130 (0.00103)	−25.2	−1.5	0	0

Adding priming to measured total respiration rate γ led to somewhat larger predicted latitudinal trend of CUE in all cases (Table 5). However, no considerable changes could be detected in the average NEP, τ or SSSC unless either priming or exudation intensity was strongly increased. Under the assumption that exuded carbon triggered a five-fold heterotroph respiration, mean NEP declined as much as 70%, leading to a 2 kg m^{-2} reduction in SSSC. In this simulation, heterotroph respiration due to priming equaled total ECM-related respiration and was about 30% of total heterotroph respiration. Increasing exudation threefold but keeping the priming parameter in its default value, led to a 40% decrease in mean NEP but no change in SSSC (Table 5).

3.3. Partitioning the causes of uncertainty in CUE estimates

More than 60% of country-level CUE uncertainty was caused by the variation of soil C:N ratio across Finland (Fig. 10b). For a given site with C:N ratio fixed to 30, half of total uncertainty for pine came from the estimation of $\frac{W_{RT}}{W_f}$, while for spruce half was from the parameter σ_C (Fig. 10d), because pine tended to have considerably higher parametric uncertainty of $\frac{W_{RT}}{W_f}$ than spruce (Fig. S4.1a). The large parametric uncertainty of the environmentally-driven structure parameters ρ_M and $\frac{W_{RT}}{W_f}$ (Fig. 4, S4.1) respectively propagated 34% and 50% of the uncertainty in the relation between CUE and ETS. The predicted relation between CUE and ETS was significantly positive, even considering the uncertainty from all parameters and empirical modules (Fig. 10e).

Pine did not show higher CUE than spruce (Fig. 10), because the positive effect of higher photosynthesis rate of pine (σ_C, Table 2) on CUE was counteracted by the negative effect of higher $\frac{W_{RT}}{W_f}$ and $\frac{W_w}{W_f}$ (Fig. S4.1).

4. Discussion

4.1. Empirically-based trends in CUE and NEP

This study utilized a unique compilation of data to establish possible trends in CUE and NEP across a latitudinal gradient. We introduced two methods, both based on theoretical analyses of forest C balance, that should give accurate results if appropriate data was available (Eqns (13) and (15)). Here, we combined various measurements and models with forest statistics to obtain a regional coverage of estimates. It is not surprising that the variance of the results was large, given that some of the data were only available as sub-region averages, while other variables came from defined data points (the Biosoil data) or from a wall-to-wall grid with specified resolution (litter fall data). Nevertheless, both methods gave comparable results, albeit Method 1 estimates were consistently slightly higher than Method 2 for both CUE and NEP.

The CUE estimates compare well with previous literature. Collalti and Prentice (2019) found in a review covering different biomes that

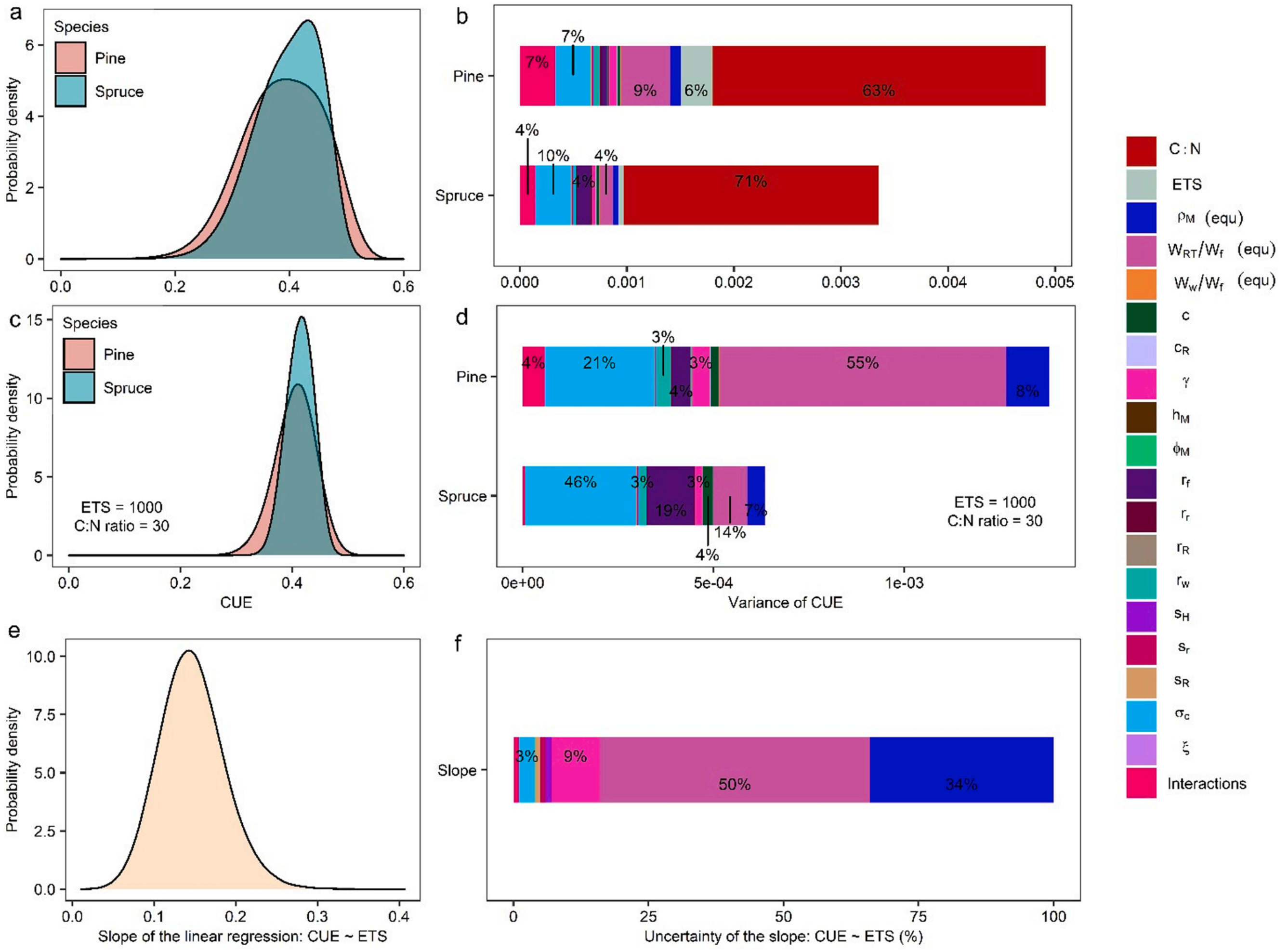

Fig. 10. Uncertainty of CUE estimates at (a, b) country level, (c, d) site-specific level, and (e, f) uncertainty of the relation between CUE and ETS. Note: Probability density was generated using Monte Carlo technique (a, c, e). The variance was partitioned using Sobol's first order indices (b, d, f). Input factors with a contribution above 3% were labelled (b, d, f). Figure e and f are for the slope parameter in the linear regression between CUE and ETS/1000. The total variance of the slope parameter was rescaled to 100% (f).

average CUE was 0.46 ± 0.12, with no apparent trend between biomes, whereas a meta-analysis by DeLucia et al. (2007) suggested differences among biomes, with mean CUE ca. 0.3 in the boreal forest. The temperature dependence of GPP and NPP estimated by West (2020) would suggest CUE of young stands to vary between 0.1 and 0.3 and of old stands between 0.05 and 0.2 within the temperature range of Finland. Our mean results fall between those of Collalti and Prentice (2019) and DeLucia et al. (2007). Our latitudinal trend is somewhat weaker than that shown by West (2020) and the absolute values of CUE are larger. These differences may be caused by the fact that our analysis included ground vegetation whereas West (2020) compared tree stand to ecosystem-level eddy-covariance based GPP. The role of ground vegetation in both GPP and NPP increases with increasing latitude as stands become sparser towards the north (Lehtonen et al. 2016a).

The latitudinal variation of NEP obtained in this study (Fig. 7) corresponds with ecosystem model projections (e.g. Holmberg et al. 2019), although direct measurements are only available at a few sites. The long-term average NEP at the SMEAR II station at latitude 61°51′N is about 200 g C m^{-2} yr^{-1} (Kolari et al. 2009), while in Sodankylä (67°21′N) it hovers around 0 g C m^{-2} yr^{-1}. Other stations at latitudes 68–69 have measured NEP over 100 g C m^{-2} yr^{-1} (Aurela et al. 2009).

The key model-based components of Methods 1 and 2 were the MODIS GPP and the mean residence time of carbon in soil, τ, calculated with Yasso15. The latitudinal trend in CUE is highly sensitive to the respective trend in GPP, as this appears in the denominator for both methods. The MODIS trend with latitude was found to be somewhat stronger than the respective trend of model-based potential photosynthetic production for fully stocked stands (Härkönen et al. 2010, Minunno et al. 2016) as it incorporates trends in both leaf area and leaf-area-specific photosynthesis. The trends in NEP strongly depend on the estimated τ (Eqn (13)). Our method of estimating heterotrophic respiration is obviously a simplification, but it should give an idea of latitudinal trends, as soil carbon was measured and the τ depended on measured litter fall and environmental drivers (Viskari et al. 2020). However, we should note that this trend is in reality also affected by trends in ECM colonization (Lindahl and Tunlid 2015), which was not explicitly accounted for here (Table 5).

4.2. Can ECM explain the observed trends?

Our ECM model predicted latitudinal and environmental (ETS and C:N ratio) trends that were surprisingly similar with the empirically based estimates (Figs. 6, 7). Out of these, the trend with C:N ratio differed most between the methods. As the model derived both the fine-root to foliage ratio and ECM colonization rate from the organic layer C:N ratio, the correlation with C:N ratio was strong. On the other hand, the empirical methods averaged regional data where ETS tightly followed latitude but C:N ratio did not (Fig. 5), so they would not have represented a C:N relationship even if it existed. However, even if good correspondence was found between our model and the empirical methods, the reasons for this need to be scrutinized against possible alternative explanations, and any uncertainties need to be considered.

The key assumption behind our modelling was that any environmental impacts on CUE and NEP are mediated through biomass proportions – both within trees and between trees and fungi – whereas all direct metabolic rates were taken to respond proportionally to environmental drivers. The environmental impacts on biomass proportions were based on measurements (Helmisaari et al. 2007, Lehtonen et al. 2016b, Ostonen et al. 2011) although their exact quantification remains uncertain, and the fungal relations only covered spruce (Fig. 4). Few data are available to evaluate the environmental responses of metabolic rates. Variability unaccounted for here could shift the predicted trend one way or another, depending on the impact (see review by Collalti and Prentice, 2019).

Our results suggest that trends in tree allometry do not give rise to trends in CUE, because opposite trends of fine roots and sapwood compensate for each other. This agrees with studies showing biomass allocation shifts from wood to fine roots when moving from higher to lower fertility (Litton and Giardina, 2008; Valentine and Mäkelä 2012). As a consequence, the CUE trends predicted by our model are fully attributable to ECM. Due to the assumptions that the fine-root to foliage ratio and the colonization rate of ECM increase with organic layer C:N ratio, the model-based CUE strongly depends on the C:N ratio (Fig. 5). Our model therefore provides a possible mechanistic explanation for the empirically-based hypothesis by Vicca et al. (2012) that fertile forests produce biomass more efficiently due to reduced C allocation to root symbionts.

As C:N ratio correlates strongly with latitude (Ostonen et al. 2011, Fig. 5), there could be some other underlying factor explaining both trends. One possible explanation could be that cellular respiration of trees and mycorrhizal fungi inhabiting cold and N and P poor soils to a larger proportion is funneled through the alternative oxidase pathway (AOP) (Angert et al. 2003) rather than through the cytochrome oxidase pathway. There is empirical evidence from an experiment in northern Sweden that fertilization decreases the share of AOP in (mycorrhizal) *Pinus sylvestris* roots but not in needles (Henriksson et al. 2019), and that mycorrhizal fungi may have very high AOX (Henriksson et al. unpublished data). This would also be in line with the observation of decreasing CUE with latitude.

4.3. What is the significance of ECM on CUE, NEP and soil carbon?

Quantitatively, the significance of the trend on CUE and NEP are determined by the biomass-specific metabolic rates and standing biomass of ECM. Here, our estimates were mostly based on the comprehensive study of Hagenbo et al. (2019) that quantified many of the parameters needed in the model. Based on this, the total cost of ECM was about 10 times that of hyphal growth / litter production (on average 75 and 7.2 g C m^{-2} yr^{-1}, respectively, corresponding to 9% and 0.9% of mean photosynthesis). Schiestl-Aalto et al. (2019) estimated the carbon allocation to ECM to be 6% of annual photosynthesis at SMEAR II, while other studies have reported values between 14 and 22% of NPP in conifer ecosystems (Leake et al. 2001, Finlay and Söderström 1992, Vogt et al. 1982, Ryan et al. 1996) and 8 – 17% of GPP in arctic tundra vegetation (Hobbie and Hobbie (2006)). Ding et al. (2021) estimated the ECM mycelia production in stands around SMEAR II to vary between 5.3 and 9.2 g C m^{-2} yr^{-1} (about 0.5 and 0.9% of GPP, respectively). A review by Ekblad et al. (2013) reported an average of 7.5 g C m^{-2} yr^{-1} in the upper 10 cm of 8 boreal forests.

The main conclusion from these quantitative results is that while the total cost of ECM is considerable and should be reflected in CUE, the litter production seems generally low compared with other sources of plant litter and would not have a marked effect on soil C accumulation unless its decomposition rate was considerably slower than the average C residence time in soil (Freschet et al. 2013, Adamczyk et al. 2019). If it was the same it would add about 0.23 kg m^{-2} to the average stand SSSC ($\tau \times$ litter production). The exudation and priming effect with our parameter values was generally sufficient to counteract this, such that SSSC was not largely affected by the inclusion of ECM in the analysis (Table 5, Fig. 8b).

The SSSC predicted by Yasso15 is on average 3.2 kg m^{-2} higher than the measurements, although it follows the same latitudinal trend. This could be because soil carbon in Yasso includes standing and fallen deadwood which was not included in the Biosoil measurements. Additional uncertainties could stem from the steady state assumption and the uncertainty of long-term litter fall rates, although the fluctuation around mean steady state in managed mature stands has been found to be less than ±10% (Liski et al. 2005). Yasso15 does not include any processes other than microbial decomposition to remove C from the soil, which could lead to overestimation if losses of C due to, e.g., leaching or mechanical soil preparation were more significant than suggested by available literature (Mjöfors et al. 2017).

Based on our results, it seems unlikely that excluding ECM in the soil model would cause any considerable overestimation of soil C. The result where SSSC was reduced by 0.85 kg m^{-2} (Table 5 "priming × 3") was achieved when priming caused an additional annual efflux that was about 50% of the level reported as hyphal respiration (γ) by Hagenbo et al. (2019) (result not shown). In order for SSSC to decline by 3.2 kg m^{-2}, the required increase of respiration would be 150%, respectively. This would reduce NEP too much to be credible in comparison with the empirically-based results.

5. Conclusions

In conclusion, our results corroborate the studies that have found ECM a significant sink of photosynthetic carbon in forests. We propose a way of accounting for this sink in models and carbon budget estimates without explicitly having to consider the complex carbon and nutrient interactions between plants and ECM. In our approach, the soil C:N ratio serves as a proxy for these interactions, driven by the benefit of nutrient acquisition due to high ECM colonization, recognizing that the benefit is greatest where nutrients are more strongly bound to soil organic matter.

Although the results are generally in line with existing measurements, many quantitative and qualitative uncertainties remain. More measurements of the carbon use of fungal symbionts in different environments and ecosystems are needed to shed more light on the role of symbionts in ecosystem carbon balance before the model of this study can be subjected to a stringent test and developed further.

Declaration of Competing Interest

The authors declare that they have no known competing financial interests or personal relationships that could have appeared to influence the work reported in this paper.

Acknowledgements

Knut and Alice Wallenberg Foundation (#2015.0047), Academy of Finland (#335958, #322066), EU H2020 (#101000289). No conflict of interest declared.

Appendix A. Supplementary material

Supplementary data to this article can be found online at https://doi.org/10.1016/j.foreco.2022.120355.

References

Adamczyk, B., Sietiö, O.M., Biasi, C., Heinonsalo, J., 2019. Interaction between tannins and fungal necromass stabilizes fungal residues in boreal forest soils. New Phytol. 223, 16–21. https://doi.org/10.1111/nph.15729.

Angert, A., Barkan, E., Barnett, B., Brugnoli, E., Davidson, E.A., Fessenden, J., Maneepong, S., Panapitukkul, N., Randerson, J.T., Savage, K., Yakir, D., Luz, B., 2003. Contribution of soil respiration in tropical, temperate, and boreal forests to the 18O enrichment of atmospheric O2. Global Biogeochem. Cycles 17 (3), n/a–n/a.

Aurela, M., Lohila, A., Tuovinen, J.-P., Hatakka, J., Riutta, T., Laurila, T., 2009. Carbon dioxide exchange on a northern boreal fen. Boreal Environ. Res. 14, 699–710.

Canarini, A., Kaiser, C., Merchant, A., Richter, A., Wanek, W., 2019. Root exudation of primary metabolites: mechanisms and their roles in plant responses to environmental stimuli. article 157 Front. Plant Sci. 10. https://www.frontiersin.org/article/10.3389/fpls.2019.00157.

Clemmensen, K.E., Bahr, A., Ovaskainen, O., Dahlberg, A., Ekblad, A., Wallander, H., Stenlid, J., Finlay, R.D., Wardle, D.A., Lindahl, B.D., 2013. Roots and associated fungi drive long-term carbon sequestration in boreal forest. Science 339, 1615–1618. https://doi.org/10.1126/science.1231923.

Collalti, A., Prentice, I.C., Polle, A., 2019. Is NPP proportional to GPP? Waring's hypothesis 20 years on. Tree Physiol. 39 (8), 1473–1483.

Collalti, A., Tjoelker, M.G., Hoch, G., Mäkelä, A., Guidolotti, G., Heskel, M., Petit, G., Ryan, M.G., Battipaglia, G., Matteucci, G., Prentice, I.C., 2020. Plant respiration, controlled by photosynthesis or biomass? Glob. Change Biol. 26 (3), 1739–1753.

DeLucia, E.H., Drake, J.E., Thomas, R.B., Gonzalez-Meler, M., 2007. Forest carbon use efficiency: is respiration a constant fraction of gross primary production? Glob. Change Biol. 13, 1157–1167. https://doi.org/10.1111/j.1365-2486.2007.01365.x.

Dewar, R.C., Medlyn, B.E., McMurtrie, R.E., 1999. Acclimation of the respiration/photosynthesis ratio to temperature: insights for a model. Glob. Change Biol. 5, 615–622.

Ding, Y., Leppälammi-Kujansuu, J., Salemaa, M., Schiestl-Aalto, P., Kulmala, L., Ukonmaanaho, L., Nöjd, P., Minkkinen, K., Makita, N., Železnik, P., Merilä, P., Helmisaari, H.-S., 2021. Distinct patterns of below- and aboveground growth phenology and litter carbon inputs along a boreal site type gradient. For. Ecol. Manage. 489, 119081.

Ekblad, A., Wallander, H., Godbold, D.L., Cruz, C., Johnson, D., Baldrian, P., Björk, R.G., Epron, D., Kieliszewska-Rokicka, B., Kjøller, R., Kraigher, H., Matzner, E., Neumann, J., Plassard, C., 2013. The production and turnover of extramatrical mycelium of ectomycorrhizal fungi in forest soils: role in carbon cycling. Plant Soil 366 (1-2), 1–27.

Finlay, R.D., Söderström, B., 1992. "Mycorrhiza and carbon flow to the soil" in Mycorrhizal Functioning, ed. M. F. Allen (New York, NY: Chapman and Hall), 134–160.

Fitter, A.H., 1991. Costs and benefits of mycorrhizas: implications for functioning under natural conditions. Experientia 47 (4), 350–355.

Freschet, G.T., Cornwell, W.K., Wardle, D.A., Elumeeva, T.G., Liu, W., Jackson, B.G., Onipchenko, V.G., Soudzilovskaia, N.A., Tao, J., Cornelissen, J.H.C., Austin, A., 2013. Linking litter decomposition of above- and below-ground organs to plant-soil feedbacks worldwide. J. Ecol. 101 (4), 943–952.

Gorka, S., Dietrich, M., Mayerhofer, W., Gabriel, R., Wiesenbauer, J., Martin, V., Zheng, Q., Imai, B., Prommer, J., Weidinger, M., Schweiger, P., 2019. Rapid transfer of plant photosynthates to soil bacteria via ectomycorrhizal hyphae and its interaction with nitrogen availability. Frontiers in microbiology 10, article 168. doi: 10.3389/fmicb.2019.00168.

Hagenbo, A., Hadden, D., Clemmensen, K.E., Grelle, A., Manzoni, S., Mölder, M., Ekblad, A., Fransson, P., Vries, F., 2019. Carbon use efficiency of mycorrhizal fungal mycelium increases during the growing season but decreases with forest age across a Pinus sylvestris chronosequence. J. Ecol. 107 (6), 2808–2822.

Härkönen, S., Pulkkinen, M., Duursma, R., Mäkelä, A., 2010. Estimating annual GPP, NPP and stem growth in Finland using summary models. Forest Ecol. Manage. 259 (3), 524–533.

Heiskanen, J., Hallikainen, V., Uusitalo, J., Ilvesniemi, H., 2018. Co-variation relations of physical soil properties and site characteristics of Finnish upland forests. article 9948 Silva Fennica 52 (3). https://doi.org/10.14214/sf.994.

Helmisaari, H.-S., Derome, J., Nojd, P., Kukkola, M., 2007. Fine root biomass in relation to site and stand characteristics in Norway spruce and Scots pine stands. Tree Physiol. 27 (10), 1493–1504.

Henriksson, N., Marshall, J., Lundholm, J., Boily, Å., Boily, J.-F., Näsholm, T., 2019. Improved in vivo measurement of alternative oxidase respiration in field-collected pine roots. Physiol. Plant. 167, 34–47. https://doi.org/10.1111/ppl.12910.

Hobbie, J.E., Hobbie, E.A., 2006. 15N content in symbiotic fungi and plants estimates nitrogen and carbon flux rates in arctic tundra. Ecology 87, 816–822. https://doi.org/10.1890/0012-9658(2006)87[816:NISFAP]2.0.CO;2.

Högberg, P., Nordgren, A., Buchmann, N., Taylor, A.F.S., Ekblad, A., Högberg, M.N., Nyberg, G., Ottosson-Löfvenius, M., Read, D.J., 2001. Large-scale forest girdling shows that current photosynthesis drives soil respiration. Nature 411 (6839), 789–792.

Holmberg, M., Aalto, T., Akujärvi, A., Arslan, A.N., Bergstrom, I., Bottcher, K., Lahtinen, I., Makela, A., Markkanen, T., Minunno, F., Peltoniemi, M., Rankinen, K., Vihervaara, P., Forsius, M., 2019. Ecosystem services related to carbon cycling - modeling present and future impacts in boreal forests. Front. Plant Sci. 10, 343–351.

Kolari, P., Kulmala, L., Pumpanen, J., Launiainen, S., Ilvesniemi, H., Hari, P., Nikinmaa, E., 2009. CO2 exchange and component CO2 fluxes of a boreal scots pine forest. Boreal Environ. Res. 14, 761–778.

Kramarenko, D., 2012. Metsämaan hiilen määrään ja sen muutokseen vaikuttavat tekijät (Factors influencing forest soil carbon stocks and their changes). MSc Thesis. Department of Forest Sciences. University of Helsinki.

Leake, J.R., Donnelly, D.P., Saunders, E.M., Boddy, L., Read, D.J., 2001. Rates and quantities of carbon flux to ectomycorrhizal mycelium following 14C pulse labeling of pinus sylvestris seedlings: effects of litter patches and interaction with a wood-decomposer fungus. Tree Physiol. 21, 71–82. https://doi.org/10.1093/treephys/21.2-3.71.

Lehtonen, A., Linkosalo, T., Peltoniemi, M., Sievänen, R., Mäkipää, R., Tamminen, P., Salemaa, M., Nieminen, T., Tupek, B., Heikkinen, J., Komarov, A., 2016a. Forest soil carbon stock estimates in a nationwide inventory: evaluating performance of the ROMULv and Yasso07 models in Finland. Geosci. Model Dev. 9, 4169–4183. https://doi.org/10.5194/gmd-9-4169-2016.

Lehtonen, A., Palviainen, M., Ojanen, P., Kalliokoski, T., Nöjd, P., Kukkola, M., Penttilä, T., Mäkipää, R., Leppälammi-Kujansuu, J., Helmisaari, H.S., 2016b. Modelling fine root biomass of boreal tree stands using site and stand variables. For. Ecol. Manage. 359, 361–369.

Leppälammi-Kujansuu, J., Salemaa, M., Kleja, D.B., Linder, S., Helmisaari, H.-S., 2014. Fine root turnover and litter production of Norway spruce in a long-term temperature and nutrient manipulation experiment. Plant Soil 374 (1-2), 73–88.

Lindahl, B.D., Tunlid, A., 2015. Ectomycorrhizal fungi – potential organic matter decomposers, yet not saprotrophs. New Phytologists 205, 1443–1447. https://doi.org/10.1111/nph.13201.

Liski, J., Palosuo, T., Peltoniemi, M., Sievänen, R., 2005. Carbon and decomposition model Yasso for forest soils. Ecol. Model. 189 (1-2), 168–182.

Litton, C.M., Giardina, C.P., 2008. Below-ground carbon flux and partitioning: global patterns and response to temperature. Funct. Ecol. 22, 941–954.

Mäkelä, A., Pulkkinen, M., Kolari, P., Lagergren, F., Berbigier, B., Lindroth, A., Loustau, D., Nikinmaa, E., Vesala, T., Hari, P., 2008. Developing an empirical model of stand GPP with the LUE approach: analysis of eddy covariance data at five contrasting conifer sites in Europe. Glob. Change Biol. 14, 98–108.

Mäkelä, A., Valentine, H.T., 2001. The ratio of NPP to GPP: Evidence of change over the course of stand development. Tree Physiol. 21 (14), 1015–1030.

Mäkipää, R., Heikkinen, J., 2003. Large-scale changes in abundance of terricolous bryophytes and macrolichens in Finland. J. Veg. Sci. 14, 497–508. https://onlinelibrary.wiley.com/doi/abs/10.1111/j.1654-1103.2003.tb02176.x.

Manzoni, S., Čapek, P., Porada, P., Thurner, M., Winterdahl, M., Beer, C., Brüchert, V., Frouz, J., Herrmann, A.M., Lindahl, B.D., Lyon, S.W., Šantrůčková, H., Vico, G., Way, D., 2018. Reviews and syntheses: Carbon use efficiency from organisms to ecosystems – definitions, theories, and empirical evidence. Biogeosciences 15 (19), 5929–5949.

Minunno, F., Peltoniemi, M., Launiainen, S., Aurela, M., Mammarella, I., Lindroth, A., Lohela, A., Minkkinen, K., Mäkelä, A., 2016. Calibration and validation of a semi-empirical flux ecosystem model for coniferous forests in the Boreal region. Ecol. Model. 341, 37–52.

Mjöfors, K., Strömgren, M., Nohrstedt, H.-Ö., Johansson, M.-B., Gärdenäs, A.I., 2017. Indications that site preparation increases forest ecosystem carbon stocks in the long term. Scand. J. For. Res. 32 (8), 717–725.

Ostonen, I., Helmisaari, H.-S., Borken, W., Tedersoo, L., Kukumägi, M., Bahram, M., Lindroos, A.-J., Nöjd, P., Uri, V., Merilä, P., Asi, E., Lõhmus, K., 2011. Fine root foraging strategies in Norway spruce forests across a European climate gradient. Glob. Change Biol. 17 (12), 3620–3632.

Penning de Vries, F.W.T., 1972. Respiration and growth. In: A.R. Rees, K.E. Cockshull, D. W. Hand, R.G. Hurd (Eds): Crop processes in controlled environments. Applied Botany Series 2: 327–347. Academic Press, London.

Running, S.W., Nemani, R.R., Heinsch, F.A., Zhao, M., Reeves, M., Hashimoto, H., 2004. A continuous satellite-derived measure of global terrestrial primary production. Bioscience 54, 547–560.

Running, S., Mu, Q., Zhao, M., 2015. MOD17A2H MODIS/Terra Gross Primary Productivity 8-Day L4 Global 500m SIN Grid V006. NASA EOSDIS Land Processes DAAC. https://doi.org/10.5067/MODIS/MOD17A2H.006.

Ryan, M.G., Hubbard, R.M., Pongracic, S., Raison, R.J., McMurtrie, R.E., 1996. Foliage, fine-root, woody-tissue and stand respiration in Pinus radiata in relation to nitrogen status. Tree Physiol. 16, 333–344. https://doi.org/10.1093/treephys/16.3.333.

Ryu, Y., Berry, J.A., Baldocchi, D.B., 2019. What is global photosynthesis? History, uncertainties and opportunities. Remote Sens. Environ. 223, 95–114. https://doi.org/10.1016/j.rse.2019.01.016.

Schiestl-Aalto, P., Ryhti, K., Mäkelä, A., Peltoniemi, M., Bäck, J., Kulmala, L., 2019. Analysis of the NSC Storage Dynamics in Tree Organs Reveals the Allocation to Belowground Symbionts in the Framework of Whole Tree Carbon Balance. Frontiers in forests and global change 2, article 17.

Talbot, J.M., Allison, S.D., Treseder, K.K., 2008. Decomposers in disguise: mycorrhizal fungi as regulators of soil C dynamics in ecosystems under global change. Funct. Ecol. 22, 955–963.

Tomppo, E., Heikkinen, J., Henttonen, H.M., Ihalainen, A., Katila, M., Mäkelä, H., Tuomainen, T., Vainikainen, N., 2011. Designing and conducting a forest inventory – case: 9th National Forest Inventory of Finland. Springer, Dordrecht, Netherlands.

Tuomi, M., Vanhala, P., Karhu, K., Fritze, H., Liski, J., 2008. Heterotrophic soil respiration-Comparison of different models describing its temperature dependence. Ecological Modelling 211, 182–190. https://doi.org/10.1016/j.ecolmodel.2007.09.003.

Tuomi, M., Laiho, R., Repo, A., Liski, J., 2011. Wood decomposition model for boreal forests. Ecol. Model. 222, 709–718. https://doi.org/10.1016/j.ecolmodel.2010.10.025.

Ťupek, B., Mäkipää, R., Heikkinen, J., Peltoniemi, M., Ukonmaanaho, L., Hokkanen, T., Nöjd, P., Nevalainen, S., Lindgren, M., Lehtonen, A., 2015. Foliar turnover rates in Finland — comparing estimates from needle-cohort and litterfall-biomass methods. Boreal Environ. Res. 20, 283–304.

Valentine, H.T., Mäkelä, A., 2012. Modeling forest stand dynamics from optimal balances of carbon and nitrogen. New Phytol. 194, 961–971.

Vanhala, P., Karhu, K., Tuomi, M., Björklöf, K., Fritze, H., Liski, J., 2008. Temperature sensitivity of soil organic matter decomposition in southern and northern areas of the boreal forest zone. Soil Biol. Biochem. 40, 1758–1764.

Vanninen, P., Mäkelä, A., 2005. Carbon budget for individual Scots pine trees: effects of size, competition and site fertility on growth allocation. Tree Physiol. 25, 17–30.

Vicca, S., Luyssaert, S., Peñuelas, J., Campioli, M., Chapin, F.S.I.I.I., Giais, P., Heinemeyer, A., Högberg, P., Kutsch, W.L., Law, B.E., Malhi, Y., Papale, D., Piao, S. L., Reichstein, M., Schulze, E.D., Janssens, I.A., 2012. Fertile forests produce biomass more efficiently. Ecology Letters 15, 520–526.

Viskari, T., Laine, M., Kulmala, L., Mäkelä, J., Fer, I., Liski, J., 2020. Improving Yasso15 soil carbon model estimates with ensemble adjustment Kalman filter state data assimilation. Geosci. Model Dev. 13, 5959–5971. https://doi.org/10.5194/gmd-13-5959-2020.

Vogt, K.A., Grier, C., Meier, C.E., Edmonds, R.L., 1982. Mycorrhizal role in net primary production and nutrient cycling in Abies amabilis ecosystems in western Washington. Ecology 63, 370–380. https://doi.org/10.2307/1938955.

Wallander, H., Göransson, H., Rosengren, U., 2004. Production, standing biomass and natural abundance of 15N and 13C in ectomycorrhizal mycelia collected at different soil depths in two forest types. Oecologia 139, 89–97.

Wang, J., Sun, J., Xia, J., He, N., Li, M., Niu, S., 2017. Soil and vegetation carbon turnover times from tropical to boreal forests. Funct. Ecol. 32, 71–82. https://doi.org/10.1111/1365-2435.12914.

Wertin, T.M., Teskey, R.O., 2008. Close coupling of whole-plant respiration to net photosynthesis and carbohydrates. Tree Physiol. 28, 1831–1840.

West, P.W., 2020. Do increasing respiratory costs explain the decline with age of forest growth rate? J. For. Res. 31, 693–712. https://doi.org/10.1007/s11676-019-01020-w.

Wieder, W.R., Allison, S.D., Davidson, E.A., Georgiou, K., Hararuk, O., He, Y., Hopkins, F., Luo, Y., Smith, M.J., Sulman, B., Todd-Brown, K., Wang, Y.-P., Xia, J., Xu, X., 2015. Explicitly representing soil microbial processes in Earth system models. Global Biogeochem. Cycles 29, 1782–1800. https://doi.org/10.1002/2015GB005188.